

Omni-3DEdit: Generalized Versatile 3D Editing in One-Pass

Liyi Chen*, Pengfei Wang*, Guowen Zhang, Zhiyuan Ma, Lei Zhang[†]
 The Hong Kong Polytechnic University
 liyi0308.chen@connect.polyu.hk, cslzhang@comp.polyu.edu.hk

Abstract

Most instruction-driven 3D editing methods rely on 2D models to guide the explicit and iterative optimization of 3D representations. This paradigm, however, suffers from two primary drawbacks. First, it lacks a universal design of different 3D editing tasks because the explicit manipulation of 3D geometry necessitates task-dependent rules, e.g., 3D appearance editing demands inherent source 3D geometry, while 3D removal alters source geometry. Second, the iterative optimization process is highly time-consuming, often requiring thousands of invocations of 2D/3D updating. We present Omni-3DEdit, a unified, learning-based model that generalizes various 3D editing tasks implicitly. One key challenge to achieve our goal is the scarcity of paired source-edited multi-view assets for training. To address this issue, we construct a data pipeline, synthesizing a relatively rich number of high-quality paired multi-view editing samples. Subsequently, we adapt the pre-trained generative model SEVA as our backbone by concatenating source view latents along with conditional tokens in sequence space. A dual-stream LoRA module is proposed to disentangle different view cues, largely enhancing our model’s representational learning capability. As a learning-based model, our model is free of the time-consuming online optimization, and it can complete various 3D editing tasks in one forward pass, reducing the inference time from tens of minutes to approximately two minutes. Extensive experiments demonstrate the effectiveness and efficiency of Omni-3DEdit. Code: <https://github.com/mt-cly/Omni3DEdit>.

1. Introduction

Instruction-based 3D editing aims to edit a given 3D asset according to user’s text prompt, encompassing tasks such as altering object appearances [23], adding new objects to specified locations [6], removing or replacing existing objects [47], etc. The predominant approach to

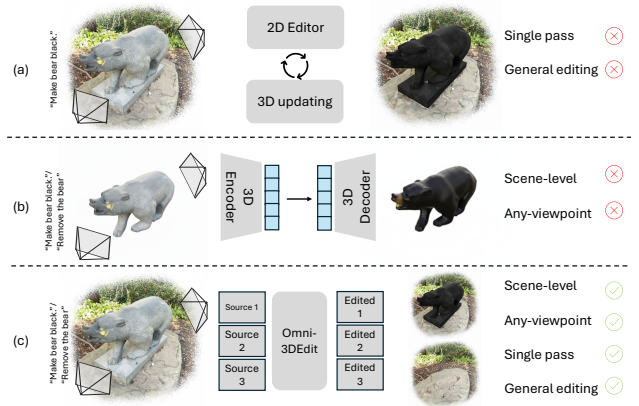


Figure 1. **Motivation of Omni-3DEdit.** (a) 3D editing via iterative 2D-3D-2D optimization with explicit 3D representation lacks generality and is time-consuming. (b) Performing 3D editing in latent space is hard to handle scene-level assets with arbitrary viewpoints. (c) Our Omni-3DEdit aims to solve these issues in multi-view space to perform fast, general, and consistent editing.

this challenge involves leveraging 2D vision-language models [22, 36, 57, 72, 74, 82] to guide the iterative refinement of a 3D representation. However, a fundamental limitation of 2D models is their lack of multi-view consistency. Existing methods [7, 11, 43, 66, 68] rely heavily on an iterative 2D-3D-2D optimization loop to alleviate the inconsistencies arising from per-view edits. For instance, to achieve 3D appearance editing, Instruct-N2N [23], DGE [11], and ViCANeRF [19] repeatedly sample camera views to compute 2D gradients, updating a NeRF [46] or Gaussian [34] representation to preserve the original consistent geometry. In parallel, 3D removal methods [15, 16, 47] often warp foreground masks and employ 2D inpainting models to fill the missing regions, which require explicit 3D updates iteratively as well.

While these methods have achieved notable success in their respective domains, they suffer from two critical drawbacks. First, these approaches are task-specific and lack generality. Appearance editing is heavily reliant on the source 3D geometry, whereas object removal requires masks and often involves large-scale geometric deforma-

*Equal contribution. [†]Corresponding author.

tions. It is difficult to design a universal iterative rule compatible with diverse editing tasks. Second, multi-round iterative process leads to excessive computation time and can over-smooth texture details. For example, InstructN2N [23] requires dozens of minutes for a single appearance edit.

We argue that maintaining and updating an explicit 3D representation, while ensuring consistency, is inherently ill-suited and slow for universal and rapid adaptation to various 3D editing commands. Although recent methods such as Tailor3D [50] and CMD [35] have explored editing in a 3D latent space [25, 84] to enable a single-pass unified framework, their models are fitted on object-centric datasets (e.g., ObjectVerse [18]), limiting them to specific camera pose distributions and rendering them incapable of handling general 3D scene inputs.

Instead, in this paper, we introduce **Omni-3DEdit**, a novel framework that addresses the above-mentioned challenges by performing 3D editing directly in the multi-view latent space, as shown in Fig. 1. Our model accepts multi-view images of the original 3D asset from arbitrary viewpoints and an editing instruction, and outputs a set of consistently edited multi-view images. Compared to paradigms that operate in explicit 3D space or on object-level 3D latents, our Omni-3DEdit takes advantage of recent advancements in multi-view generation, 2D editing, and 3D reconstruction. Specifically, we first employ VGGT [62] to acquire camera cues for the input views, which is crucial for ensuring multi-view consistency. We then obtain the reference view by using the recent single-image editor Qwen-Image [69] to perform instruction-guided editing on a randomly selected source view. Subsequently, we introduce OmniNet, a model trained to propagate this edited view consistently across the other viewpoints. OmniNet takes the camera poses, the source multi-view images, and the reference image as input to synthesize remaining edited views. Finally, the resulting view set can be fed into a reconstruction model (e.g. AnySplat [30]) to obtain edited 3D asset.

To overcome the scarcity of large-scale paired training data for this task, we adopt a two-pronged strategy. First, we leverage the consistency priors of existing multi-view models to build an offline data synthesis pipeline [30, 69], generating paired training data for various tasks, including 3D removal, addition, and appearance editing. Second, we repurpose the pre-trained multi-view generative model SEVA [89] to reduce data dependency. A dual-stream LoRA [26] module, composing of *Geometry LoRA* and *Guidance LoRA*, is trained to encode the source and target views, preventing the model from disregarding the crucial geometric priors of the source asset.

In summary, our contributions are threefold. First, we propose Omni-3DEdit, a learning-based framework that operates in the multi-view latent space, enabling single-pass, efficient, and unified editing for diverse, scene-level 3D as-

sets. Second, we explore and present effective strategies for training a multi-view consistent editing model *OmniNet* in data-constrained scenarios. Third, extensive experiments demonstrate the superior efficiency and effectiveness of our proposed method in various 3D editing tasks.

2. Related Work

3D Editing in 3D Representation Space. Early works aimed to achieve instruction-driven 3D editing by coupling existing 2D multi-modal generation or editing models with 3D representations such as NeRF [46] or Gaussian Splatting [34]. On one hand, the 2D multi-modal models provide a robust text comprehension interface and editing guidance [10, 37], while the 3D representation ensures that the editing results adhere to 3D geometry. To ensure multi-view consistency, most methods iteratively evoke 2D models and 3D representations. InstructN2N [23], GaussianEditor [71] and the following works [60, 61, 66, 90] convey view-dependent denoising gradient into 3D representations, iterating thousands of times to achieve appearance editing. While object removing and inpainting methods [6, 14, 47] share a similar workflow based on 2D inpainters, these methods need to maintain a 3D representation during the editing process and update it in an optimization-based manner. In summary, this category of approaches lacks compatibility across different editing tasks and is highly time-consuming.

3D Editing in Object-level 3D Latent Space. Leveraging pre-trained object-level 3D generative models (e.g. Shape-E [32], LRM [25], and GS-LRM [84]), methods in [3, 12, 35, 50, 78] explore learning an editing mapping within the latent space of the 3D representation. Compared to maintaining an explicit 3D representation, the latent space is easier to be integrated into editing networks, making it possible to learn a direct mapping from the original 3D latent to the edited latent. However, these methods require view inputs from specific object-centered camera poses and they are constrained by the limitations of base 3D generation model, which can only handle background-free 3D objects [18]. As a result, these methods cannot process scene-level editing from arbitrary viewpoints.

3D Editing in Video/Multi-view Latent Space. Some methods use pre-trained video generation models [4, 24, 59, 75–77] to predict edited multi-views within the RGB space across consecutive frames. The generative video models enable the handling of scene-level 3D editing. DGE [11], EditCast3D [51], and V2Edit [85] introduce video editing for 3D editing. However, video generation models suffer from (1) a weak prior for 3D consistency, (2) the need for continuous viewpoint transformations, which is computationally expensive, and (3) a lack of understanding camera poses, resulting in suboptimal performance in both computational efficiency and editing quality. DiGA3D [48],

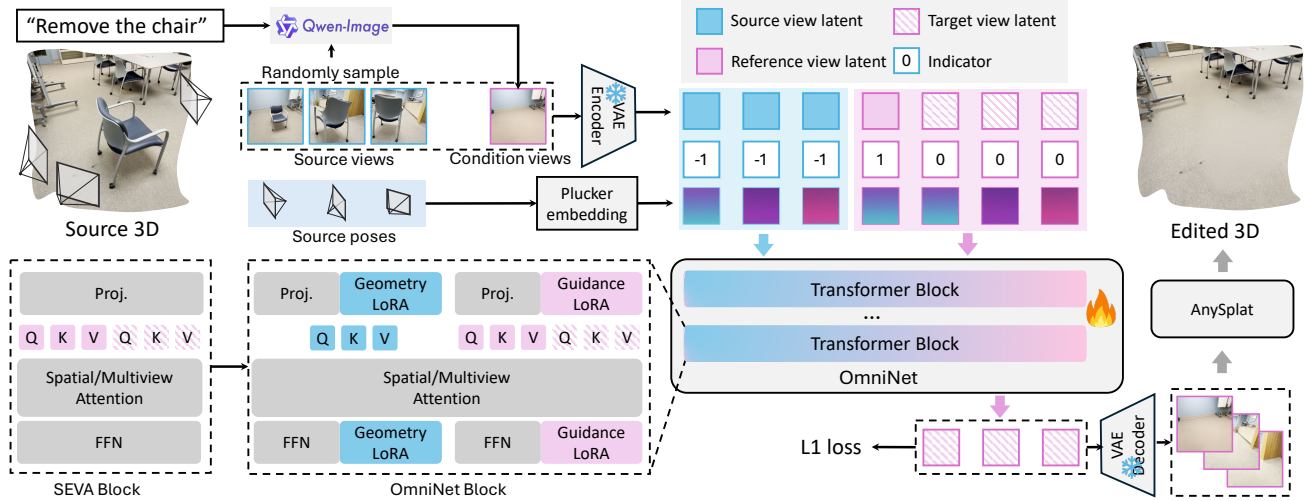


Figure 2. **Overview of Omni-3DEdit.** Given the instruction and multi-view images as inputs, we first employ Qwen-Image to obtain an edited reference image as condition view. Then an OmniNet is trained to map the editing cues from condition view to other views. The outputs of OmniNet are edited multi-view images, which can be used to obtain the edited 3D asset optionally.

Pro3D-Editor [88], and methods [1, 54, 58] share a similar idea of studying editing in multi-view latent space. They fall into the per-scene-optimization paradigm for specific editing tasks. Concurrent work Tinker [87] fails to tackle 3D editing that involves significant geometry changes, such as removal or addition. Instead, our Omni-3DEdit achieves unified and generalized 3D editing.

3. Method

Our Omni-3DEdit firstly leverages the 2D multimodal editor Qwen-Image [69] to perform instruction-based editing on an image from a randomly selected view, obtaining a *edited reference image* as the condition. Then, an *OmniNet* is introduced and trained to propagate the edited cues to the other source views. This paradigm not only takes advantage of the recent progress in 2D editing models but also reduces data and resource consumption, so that the OmniNet can focus exclusively on learning within the vision modality. In this section, we first describe the overview of Omni-3DEdit in Sec. 3.1 and then introduce the pipeline to generate paired training data in Sec. 3.2. The proposed dual-stream LoRA for training OmniNet is elaborated in Sec. 3.3.

3.1. Overview of Omni-3DEdit

As shown in Fig. 2, given N source view inputs $I_{src} = \{I_{src}^1, I_{src}^2, \dots, I_{src}^N\}$ from the source 3D scene and the editing instruction prompt P , we first employ VGGT [62] to obtain their relative camera poses $p = \{p^1, p^2, \dots, p^N\}$. Then, we randomly select a view from the input views and edit it using off-the-shelf Qwen-Image [69], obtaining a conditional image I_{cond} to provide editing cues. These images are fed into a VAE encoder [53] to produce the source view

latents $s = \{s^1, s^2, \dots, s^N\}$ and the condition view latent c .

During the training phase, noisy target latents $y_\sigma = \{y_\sigma^1, y_\sigma^2, \dots, y_\sigma^N\}$ are obtained following EDM [33]:

$$y_\sigma^n = y^n + \sigma\epsilon, \quad (1)$$

where y^n , σ , and ϵ are the n -th clear target view latent, noise level, and random noise, respectively. We concatenate the triplet latents s , c , and y_σ in sequence space to avoid introducing an extra module, taking full advantage of the pre-trained prior for understanding geometry relations among views. To distinguish the different latents, s , c , and y_σ receive -1, 1, and 0 indicators in feature space, respectively. Besides, to supplement the perspective geometry relations among views, p of source views are converted into Plücker embeddings and conveyed to the condition view and noisy target views in the feature space. These input cues are fed into OmniNet $f(\cdot)$ to perform sample prediction. Similar to the training paradigm of SEVA [89], the loss is calculated only for the latents of target views, as shown below:

$$\mathcal{L} = \mathbb{E} \left[\|f(y_\sigma, s, c, \sigma) - y\|_2^2 \right]. \quad (2)$$

During the inference stage, the edited views can be interpolated by feeding the denoised target latent into VAE decoder. AnySplat [30] is optional to obtain edited 3D assets based on edited multi-view in seconds.

Note that Omni-3DEdit makes no assumptions about task priors. Instead, the model needs to implicitly learn to propagate the edit content solely based on the relationship between the reference and source views, thereby ensuring compatibility with versatile tasks.

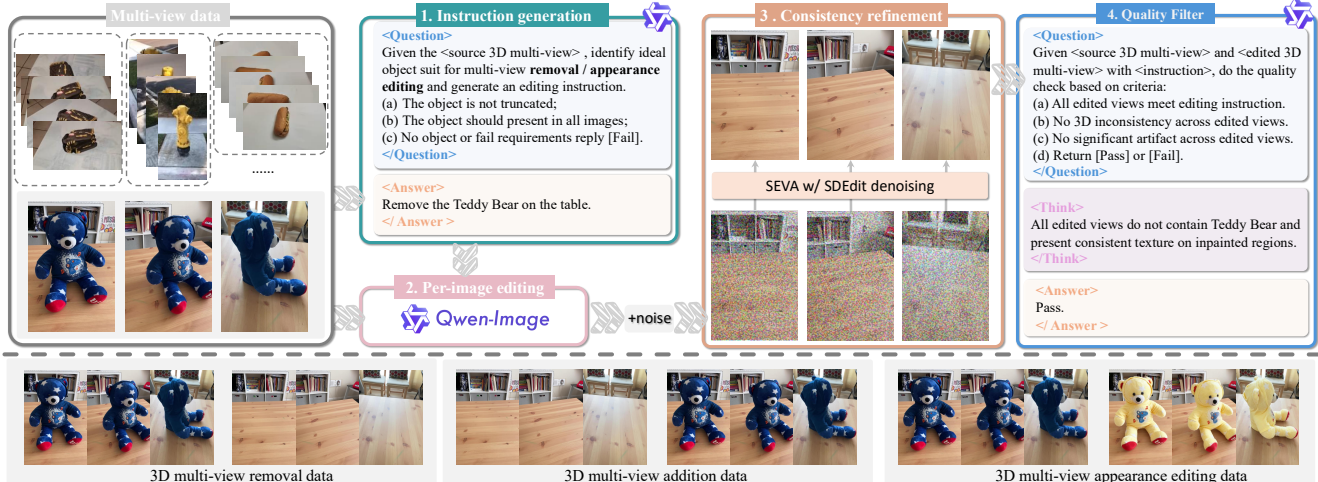


Figure 3. **Data Construction Pipeline.** The original multi-view images are passed through a four-stage pipeline to obtain their paired multi-view counterparts after editing. The pipeline covers tasks of 3D removal, addition, and appearance editing.

3.2. Paired Training Data Generation

To drive OmniNet training, we require a dataset of paired 3D multi-view images before and after editing, which should cover diverse scenes and various editing tasks. Given the scarcity of publicly available large-scale scene-level editing datasets, we focus on three common editing categories: 3D addition, 3D removal, and appearance editing. Leveraging existing open 3D multi-view datasets, we establish a data pipeline that integrates existing tools to batch-generate the desired samples for training. Our key insight lies in the observation that both per-view 3D removal and appearance editing usually involve slight multi-view texture inconsistency, which can be alleviated via consistency refinement, while 3D addition data can be obtained by inverting the source and edited views of 3D removal data.

3D Removal. The pipeline is illustrated in Fig. 3, which includes 4 steps. (1) *Instruction generation.* Given multiple source views, we first employ Gemini-2.5pro [17] to analyze and identify an ideal object for deletion, and concurrently generate a textual editing instruction. Suitable candidates are defined as objects that have clear boundaries, are not truncated, and remain consistently visible across all views. (2) *Per-image editing.* We utilize Qwen-Image [69] to perform per-view foreground removal with generated instructions. (3) *Consistency refinement.* To alleviate inconsistencies introduced by per-view editing (e.g., object-removed background regions exhibit disparate textures or colors), inspired by SDEdit [45], we introduce light-intensity (20%) noise to all edited views and then denoise them using the pre-trained SEVA [89]. (4) *Quality filter.* Due to the inherent stochasticity of 2D editing models and the varying difficulty of editing certain objects, which can lead to undesirable results, we implement an additional

Table 1. **Statistics of paired edited multi-views** in our curated training set, categorized by dataset and edit type.

Editing Type	CO3Dv2 [52]	DL3DV [40]	WildRGB-D [73]
3D Addition	15K	7K	6K
3D Removal	15K	6K	6K
3D Appearance Editing	13K	5K	5K

quality assessment to filter out undesired or failed samples. **3D Appearance Editing.** Similar to the 3D removal task, appearance editing presents challenges in maintaining visual consistency across views when they are edited frame-by-frame. These inconsistencies manifest with variations in texture and color. Fortunately, such issues can be effectively addressed through the consistency refinement step in our 3D removal data pipeline.

3D Addition. In contrast to 3D removal and appearance editing, 3D addition introduces severe geometric inconsistencies across the edited views, which cannot be effectively alleviated through consistency refinement. Therefore, we adopt a reverse strategy for data generation. Specifically, we utilize the original 3D multi-view images as the target views, and subsequently use the outputs from our 3D removal data pipeline as the corresponding source views. This methodology ensures that the ground-truth target views are inherently multi-view consistent. This strategy is similar to VIVID-10M [27], but we do not need extra masks [8, 9, 81, 83].

Statistics of Constructed Training Pairs. With the training data generation pipeline, We construct training data based on three off-the-shelf multi-view datasets: CO3Dv2 [52], DL3DV [40], and WildRGB-D [73], to cover a diverse range of 3D scenes from both indoor and outdoor. For each dataset, we begin by uniformly sampling scenes

Table 2. Quantitative comparison (PSNR \uparrow / LPIPS \downarrow) of 360° 3D removal methods on the 360-USID dataset.

Methods	Carton	Cone	Cookie	Newcone	Plant	Skateboard	Sunflower	Average
SPIn-NeRF [47]	16.659 / 0.539	15.438 / 0.389	11.879 / 0.521	17.131 / 0.519	16.850 / 0.401	15.645 / 0.675	23.538 / 0.206	16.734 / 0.464
2DGS + LaMa [29, 56]	16.433 / 0.499	15.591 / 0.351	11.711 / 0.538	16.598 / 0.670	14.491 / 0.564	15.520 / 0.639	23.024 / 0.194	16.195 / 0.494
2DGS + LeftRefill [5, 29]	15.157 / 0.567	16.143 / 0.372	12.458 / 0.526	16.717 / 0.677	12.856 / 0.666	16.429 / 0.634	24.216 / 0.181	16.282 / 0.518
LeftRefill [5]	14.667 / 0.560	14.933 / 0.380	11.148 / 0.519	16.264 / 0.448	16.183 / 0.463	14.912 / 0.572	18.851 / 0.331	15.280 / 0.468
Gaussian Grouping [79]	16.695 / 0.502	14.549 / 0.366	11.564 / 0.731	16.745 / 0.533	16.175 / 0.440	16.002 / 0.577	20.787 / 0.209	16.074 / 0.480
GScream [65]	14.687 / 0.587	14.655 / 0.476	12.733 / 0.429	13.662 / 0.605	16.238 / 0.437	12.941 / 0.626	18.470 / 0.436	14.758 / 0.514
Infusion [41]	14.191 / 0.555	14.163 / 0.439	12.051 / 0.486	9.562 / 0.624	16.127 / 0.406	13.624 / 0.638	21.195 / 0.238	14.416 / 0.484
Aurafusion360 [70]	17.675 / 0.473	15.626 / 0.332	12.841 / 0.434	17.536 / 0.426	18.001 / 0.322	17.007 / 0.559	24.943 / 0.173	17.661 / 0.388
Omni-3DEdit (Ours)	18.578 / 0.452	16.296 / 0.360	13.183 / 0.465	17.829 / 0.336	17.598 / 0.411	16.764 / 0.521	23.801 / 0.224	17.722 / 0.395

across different categories. From each selected scene, we randomly sample 20 images as training views. The final number of paired images in our training set is shown in Tab. 1. Note that due to the high complexity of the scenes in DL3DV and WildRGB-D, relatively fewer samples passed this quality filtering, resulting in fewer training pairs from these sources. During the training phase, we sample the editing tasks and scenes uniformly.

3.3. Dual-stream LoRA

With the constructed paired data, we repurpose SEVA [63, 89] as our editing model OmniNet, and finetune it to achieve multi-view editing by receiving additional source view latents s alongside the reference (condition) latent c and target view latents y_σ . To incorporate source view cues, there are two typical manners of feature-space concatenation and sequence-space concatenation, which have been adopted in previous novel view generation studies [2, 80]. However, we observe a significant performance degradation for these two architectures. As shown in Fig. 7, repurposed SEVA not only loses generative capability in target regions but also fails to preserve the unedited context from the source view.

We attribute this phenomenon to the use of shared projection layer for processing functionally distinct inputs. First, the source views and condition view serve different purposes. The condition view provides a precise editing signal from a specific perspective, whereas the source view provides comprehensive original context and texture information across camera poses. Forcing OmniNet to process these functionally dissimilar latents with shared layers introduces a learning conflict. Second, the shared weights lack the ability to differentiate bias signals across blocks, so that the model has to distinguish source and condition latents by mapping them to different feature spaces. This mechanism is ineffective in helping the target latent to correctly identify and utilize the source latent features.

Therefore, as shown in Fig. 2, we modify the architecture of SEVA to maintain two distinct sets of parameters within each block to individually encode the source latent and the condition latent. Specifically, OmniNet is based on the pre-trained linear layers of SEVA and introduces a dual-stream LoRA [26] module, including a geometry LoRA to process s to capture geometry priors among source views,

and a guidance LoRA to propagate editing guidance from c to y_σ . The features from dual streams will exchange geometry cues and editing guidance in shared multi-view attention layers. This distengled mechanism not only enables OmniNet to learn specialized representations from different views but also introduces a crucial inductive bias, which ensures that the target latent can correctly identify and attend to the features from both view latents.

Discussion. Note that compared to MM-DiT [20], our proposed dual-stream LoRA has two notable distinctions. First, MM-DiT maintains two independent sets of full parameters, but our method utilizes parameter-efficient LoRA modules. This allows OmniNet to leverage the priors of SEVA without full-scale duplication. Second, MM-DiT is designed to handle inputs from different modalities (*e.g.*, text and image). In contrast, we prove that such a dual-stream paradigm is effective for inputs of the same modality (*i.e.*, vision latents) that serve distinct roles.

4. Experiment

4.1. Experiment Setup

Implementation Details. For preprocessing, we follow the pipeline from SEVA [89], normalizing cameras within the same scene to the coordinate range of $[-2, 2]$ and setting $N = 10$. The LoRA rank is set to 8. We train OmniNet for 4,000 iterations with batch size of 32, distributed across 16 NVIDIA H20 GPUs. The number of multi-view denoising steps is set to 50. All images are processed at a resolution of 576×576 . We utilize the AdamW [42] optimizer with a constant learning rate of 1×10^{-4} with Eps-weighting MSE loss. We follow SEVA [89] to use SNR shift.

Evaluation Datasets. While Omni-3DEdit can tackle Versatile tasks in an unified manner, we compare it with specific methods respectively. For 3D removal, we utilize the unbounded 360 scene dataset, 360-USID [70], which contains seven 360-degree scenes, comprising three indoor and four outdoor environments. For 3D addition, we follow MVInpainter [6] to study the NVS performance on CO3Dv2 [52] validation set with sampling one scene per object. For 3D appearance editing, we omit numerical results due to the lack of publicly available benchmarks. Instead, we collect a series of complex 3D editing

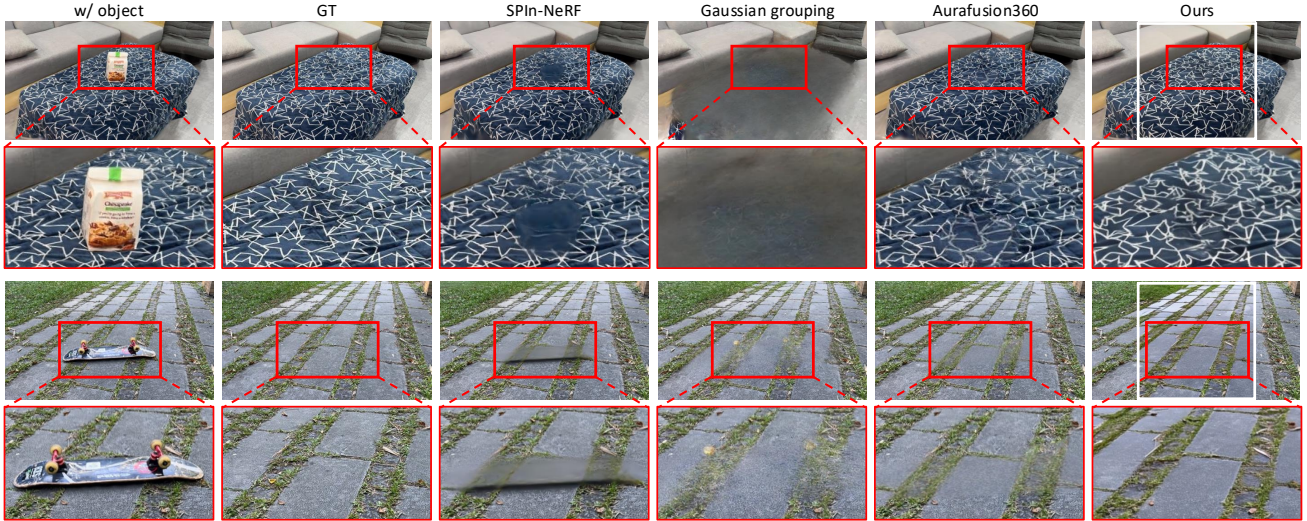


Figure 4. **Qualitative comparisons to 3D removal methods.** Our Omni-3DEdit not only removes the specific object completely but also presents rich details in the removed regions compared to other methods. We center crop views to adapt OmniNet resolution (white box).

cases involving multi-round editing or significant geometry changes to compare the performance of different methods.

Metrics. We use PSNR, and LPIPS as our evaluation metrics on 3D removal and addition. Following the protocol in prior work [47], we compute these metrics only within the object mask to more accurately evaluate the result of 3D removal. Besides, we introduce CLIP text-image score, CLIP directional score to study the editing quality on our curated test set. In addition, we leverage mLLM Gemini-2.5pro [17] to conduct a more comprehensive evaluation on the 3D editing quality. Please refer to **Supplementary File** for more details.

4.2. Experimental Results

3D Removal. Omni-3DEdit is directly applicable to the 3D removal task. By using a 2D editor to perform object erasure on an arbitrary single view, we acquire a reference anchor view. OmniNet can then generate all remaining views. Note that our method operates in a mask-free manner, in contrast to prior works such as MVInpainter [6], SPIn-NeRF [47], and Aurafusion360 [70], which need multi-view object masks to localize the target regions.

We first conduct a quantitative evaluation on the 360-USID dataset [70], comparing our method against specialized 3D removal baselines, including 2DGS [29] + LeftRe-fill [5], GScream [65], and SPIn-NeRF [47]. As demonstrated in Tab. 2, our method achieves superior 3D removal performance. Compared to Aurafusion360 [70], our approach achieves an advantage in PSNR and costs much less time (2min *v.s.* 30min) since Omni-3DEdit is free of iterative warping and obtains edited multi-view in a single pass.

We then provide qualitative comparisons in Fig. 4 to illustrate the superiority of our approach. One can observe

Table 3. **Quantitative comparison on CO3Dv2 val set.**

Method	PSNR \uparrow	LPIPS \downarrow	CLIP-T \uparrow
ZeroNVS [55]	14.56	0.716	0.196
MVInpainter [6]	19.20	0.344	0.271
Omni-3DEdit (Ours)	20.67	0.278	0.277

that compared to Gaussian Grouping [79], Omni-3DEdit correctly identifies the target object for removal without corrupting the content of adjacent objects (*e.g.*, the desk). Furthermore, regarding the visual quality of object-removed regions, Aurafusion360 [70] exhibits significant artifacts and residual contours at the object boundaries, while our method demonstrates a clear advantage in maintaining high-fidelity and consistent details.

3D Addition. To validate the model’s capability for 3D object addition, we follow the evaluation methodology established by MVInpainter [6], utilizing the multi-view images from the CO3Dv2 [52] validation set. For each scene, we retain an arbitrary view as the reference image, while the foreground objects in all remaining views are erased and inpainted via Qwen-Image. OmniNet is employed to generate these erased objects conditioned on the reference image, where the target object visible. This experimental setup is to investigate the novel view synthesis (NVS) capability in the context of object addition. As shown in Tab. 3, ZeroNVS [55] fails to fully take the context from source views and generates target views based on the single reference view, achieving the worst performance. MVInpainter [6] heavily relies on complex pre-processing (*e.g.*, point matching, mask propagation), limiting its generalization ability and achieving sub-optimal performance. Our Omni-3DEdit learns the mapping from source views to target edited views and outperforms MVInpainter in synthe-



Figure 5. **Comparison of 3D appearance editing.** Red box represents the reference view. White boxes are object masks as additional inputs for MVinpainter.

sized novel view quality. Omni-3DEdit is built upon SEVA, thereby inheriting its original ability for consistent generation under specified camera poses.

3D Appearance Editing. We further demonstrate the applicability of our method to 3D appearance editing. Despite relying on a single reference image that often offers limited-view guidance, Omni-3DEdit implicitly captures instance-level geometric priors, allowing it to effectively propagate editing signals to other regions unobserved in the reference view. We illustrate this capability with showcase of “*Make bear black.*” [23], a scene out of our training data. As shown in Fig. 5, while the reference image solely presents the left perspective, Omni-3DEdit successfully propagates the editing guidance to the entire bear instance, including its rear view. In contrast, prior reference-based 3D editing methods often struggle with 360° appearance editing. This limitation stems from their either heavy reliance on depth warping [64], which fails to handle accumulated errors across large viewpoint changes [21, 44], or their need for explicit masks for instance identification, resulting in the corruption of original geometric information [6, 44]. As demonstrated in the second row, MVinpainter fails to preserve the original geometry, yielding unsatisfactory results.

Complex 3D Editing. Our method supports fundamental operations, including 3D removal, 3D addition, and appearance editing. By combining them, we can achieve more complex editing tasks such as replacement and multi-turn editing. We collect a test benchmark to study the performance of Omni-3DEdit on such tasks. More details can be found in the **Supplementary File**.

As shown in Tab. 4, Omni-3DEdit presents significant advantages over previous methods in terms of both Gemini score and time cost. This is mainly due to fact that previous studies can only tackle specific editing tasks such as appearance editing. In addition, they heavily rely on iteratively evoking the 2D editor and explicit 3D representations, resulting in long convergence.

Table 4. **Comparison of methods on complex 3D editing.**

Method	CLIP-T/I	CLIP-Dir.	Gemini score	Time
DGE [11]	0.246	0.132	1.7	5min
GaussianEditor [13]	0.253	0.146	2.0	17min
ViCANeRF [19]	0.257	0.141	2.2	28min
Nano-banana [17]	0.281	0.165	3.8	-
Omni-3DEdit (Ours)	0.286	0.170	4.0	2min



Figure 6. **Results of competing 3D editing methods for a complex task “Removing the book.” then “Adding an apple to desk.”**

We present a showcase of “*Removing the book.*” then “*Adding an apple to desk.*” in Fig. 6. DGE [11] fails to achieve clear 3D editing because it relies on the source geometry to find pixel correspondences. Similar failures occur for GaussianEditor [13], although it is equipped with the more powerful editor, Nano-banana [17]. Since each edit might place the apple in a different position on the table, this makes it difficult for the explicit 3D Gaussian to converge, resulting in obvious artifacts. In Nano-banana, we concatenate the source views into a single image, utilizing its in-context capability [86] to edit multi-view at once, thereby improving their 3D consistency. However, the apples in edited views still suffer from inconsistent scale and position. In comparison, Omni-3DEdit maintains high consistency throughout this two-stage editing (removal results are shown in the right-bottom of last column), as evidenced by the coherence of wall tile textures and apple details.

4.3. Ablation Study

Architecture. We first investigate the impact of architectural choices on model performance by comparing our OmniNet, which is built upon sequence concatenation with dual-stream LoRA, with three distinct approaches that incorporate original images. (a) *SEVA zeroshot*: dropping the source view and only feeding the reference view and Gaussian noises to pre-trained SEVA to obtain generated

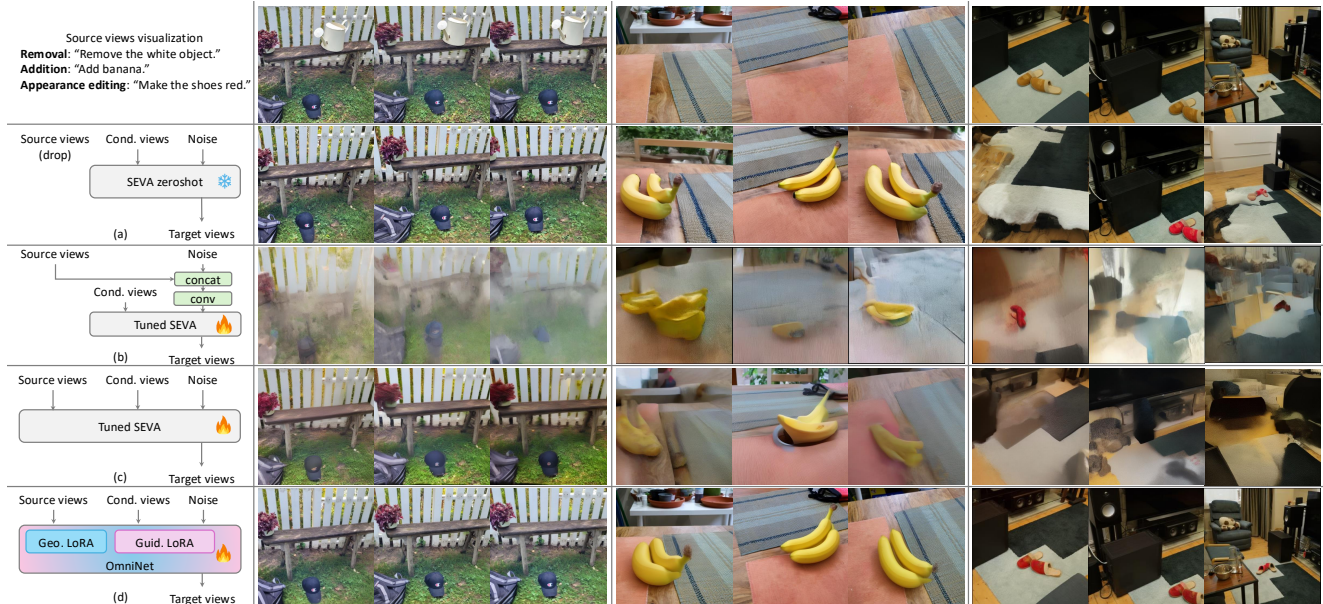


Figure 7. **Ablation study of different architectures on performing multiview editing with edited reference view.** Both plain feature-space concatenation and sequence-space concatenation fail to achieve desired editing results, while dual-stream LoRA improves the editing quality significantly. We provide edited multi-view here, and the edited 3D assets can be found in the [Supplementary File](#).

views under given camera poses. (b) *Feature-space concatenation* [80]: concatenating each Gaussian noise with its corresponding source view latent along the channel dimension, followed by feature fusion via a lightweight projection network. (c) *Sequence-space concatenation* [2, 31]: concatenating the source view latent, condition view latent, and Gaussian noises along the sequence dimension, they share the same linear layers in each block.

We provide visualization comparisons over three editing showcases provided in Fig. 7. One can observe that SEVA zero-shot fails to align source view poses since the reliance on single conditional view and normalized camera poses makes SEVA scale-agnostic during the generation process. Feature-space concatenation tends to produce obvious artifacts with blurred details. We suspect it is caused by the fact that the light convolution layers are difficult to fuse cues from source views and target views, and the cues from source view latents are vanishing when passing through the network. A similar phenomenon of bypassing source view information is also observed in sequence-space concatenation. This reveals the difficulty for pre-trained parameters to simultaneously encode both source and target views, which provide distinct information. By introducing dual-stream LoRA, OmniNet brings performance improvement by capturing geometry cues and editing guidance from source and condition views via decoupled LoRA parameters.

Input Signal. Furthermore, we investigate the critical importance of input signals for OmniNet. We conduct ablation studies by dropping the indicator and camera pose to ob-

Table 5. **Ablation study on 360-USID benchmark.**

Settings	SSIM \uparrow	PSNR \uparrow	LPIPS \downarrow
Omni-3DEdit	0.925	17.72	0.395
SEVA zeroshot	0.911	13.99	0.575
Omni-3DEdit w/o indicator	0.917	15.20	0.545
Omni-3DEdit w/o pose	0.903	14.54	0.565

serve their respective impacts on model performance. Experiments on the 360-USID benchmark [70], as presented in Tab. 5, reveal that performance degrades drastically without the indicator due to the lack of explicit signals distinguishing different views. Similarly, excluding camera poses leads to a significant performance drop, since relying solely on appearance to analyze perspective geometric information is too implicit for the model to effectively comprehend.

5. Conclusion

In this paper, we proposed Omni-3DEdit, a unified and generalized model capable of handling 3D removal, addition, and appearance editing without relying on additional masks or point matching signals. Specifically, we constructed high-quality paired edited multi-view data across different editing tasks and introduced a dual-stream LoRA module to repurpose the pre-trained multi-view generation model SEVA into a multi-view editing model, OmniNet. Extensive experiments on 3D removal, addition, and appearance editing tasks demonstrated that our Omni-3DEdit performs significantly better than existing schemes, showing strong generalization performance with much faster speed.

Limitations. Due to the scarcity of open-source scene-level multi-view data and computational resource constraints, the scale (0.1M) of our constructed dataset is relatively small, which limits Omni-3DEdit’s ability to handle very fine-grained editing tasks (e.g., “adding a bracelet to a human wrist”). A potential solution is to develop a more sophisticated data construction pipeline to generate a larger corpus of training data. In further, we plan to elaborate Omni-3DEdit with 3D agent [28, 38, 39, 83] or extend it into 4D paradigm [49, 67].

References

- [1] Hadi Alzayer, Yunzhi Zhang, Chen Geng, Jia-Bin Huang, and Jiajun Wu. Coupled diffusion sampling for training-free multi-view image editing. *arXiv preprint arXiv:2510.14981*, 2025. 3
- [2] Jianhong Bai, Menghan Xia, Xiao Fu, Xintao Wang, Lianrui Mu, Jinwen Cao, Zuozhu Liu, Haoji Hu, Xiang Bai, Pengfei Wan, et al. Recammaster: Camera-controlled generative rendering from a single video. *arXiv preprint arXiv:2503.11647*, 2025. 5, 8
- [3] Roi Bar-On, Dana Cohen-Bar, and Daniel Cohen-Or. Editp23: 3d editing via propagation of image prompts to multi-view. *arXiv preprint arXiv:2506.20652*, 2025. 2
- [4] Andreas Blattmann, Tim Dockhorn, Sumith Kulal, Daniel Mendelevitch, Maciej Kilian, Dominik Lorenz, Yam Levi, Zion English, Vikram Voleti, Adam Letts, et al. Stable video diffusion: Scaling latent video diffusion models to large datasets. *arXiv preprint arXiv:2311.15127*, 2023. 2
- [5] Chenjie Cao, Yunuo Cai, Qiaole Dong, Yikai Wang, and Yanwei Fu. Leftrefill: Filling right canvas based on left reference through generalized text-to-image diffusion model. In *Proceedings of the IEEE/CVF Conference on Computer Vision and Pattern Recognition*, 2024. 5, 6
- [6] Chenjie Cao, Chaohui Yu, Fan Wang, Xiangyang Xue, and Yanwei Fu. Mvinpainter: Learning multi-view consistent inpainting to bridge 2d and 3d editing. *arXiv preprint arXiv:2408.08000*, 2024. 1, 2, 5, 6, 7
- [7] Jun-Kun Chen, Samuel Rota Bulò, Norman Müller, Lorenzo Porzi, Peter Kotschieder, and Yu-Xiong Wang. Consistdreamer: 3d-consistent 2d diffusion for high-fidelity scene editing. In *Proceedings of the IEEE/CVF Conference on Computer Vision and Pattern Recognition*, pages 21071–21080, 2024. 1
- [8] Liyi Chen, Weiwei Wu, Chenchen Fu, Xiao Han, and Yuntao Zhang. Weakly supervised semantic segmentation with boundary exploration. In *European conference on computer vision*, pages 347–362. Springer, 2020. 4
- [9] Liyi Chen, Chenyang Lei, Ruihuang Li, Shuai Li, Zhaoxiang Zhang, and Lei Zhang. Fpr: False positive rectification for weakly supervised semantic segmentation. In *Proceedings of the IEEE/CVF international conference on computer vision*, pages 1108–1118, 2023. 4
- [10] Liyi Chen, Ruihuang Li, Guowen Zhang, Pengfei Wang, and Lei Zhang. Fast multi-view consistent 3d editing with video priors. *arXiv preprint arXiv:2511.23172*, 2025. 2
- [11] Minghao Chen, Iro Laina, and Andrea Vedaldi. Dge: Direct gaussian 3d editing by consistent multi-view editing. In *European Conference on Computer Vision*, pages 74–92. Springer, 2024. 1, 2, 7
- [12] Minghao Chen, Junyu Xie, Iro Laina, and Andrea Vedaldi. Shap-editor: Instruction-guided latent 3d editing in seconds. In *Proceedings of the IEEE/CVF Conference on Computer Vision and Pattern Recognition*, pages 26456–26466, 2024. 2
- [13] Yiwen Chen, Zilong Chen, Chi Zhang, Feng Wang, Xiaofeng Yang, Yikai Wang, Zhongang Cai, Lei Yang, Huaping Liu, and Guosheng Lin. Gaussianeditor: Swift and controllable 3d editing with gaussian splatting. In *Proceedings of the IEEE/CVF Conference on Computer Vision and Pattern Recognition*, pages 21476–21485, 2024. 7
- [14] Yuxin Cheng, Binxiao Huang, Taiqiang Wu, Wenyong Zhou, Chenchen Ding, Zhengwu Liu, Graziano Chesi, and Ngai Wong. Perspective-aware 3d gaussian inpainting with multi-view consistency. *arXiv preprint arXiv:2510.10993*, 2025. 2
- [15] Yuxin Cheng, Binxiao Huang, Taiqiang Wu, Wenyong Zhou, Chenchen Ding, Zhengwu Liu, Graziano Chesi, and Ngai Wong. Perspective-aware 3d gaussian inpainting with multi-view consistency. *arXiv preprint arXiv:2510.10993*, 2025. 1
- [16] Yuxin Cheng, Binxiao Huang, Taiqiang Wu, Wenyong Zhou, Chenchen Ding, Zhengwu Liu, Graziano Chesi, and Ngai Wong. Perspective-aware 3d gaussian inpainting with multi-view consistency. *arXiv preprint arXiv:2510.10993*, 2025. 1
- [17] Gheorghe Comanici, Eric Bieber, Mike Schaekermann, Ice Pasupat, Noveen Sachdeva, Inderjit Dhillon, Marcel Blisstein, Ori Ram, Dan Zhang, Evan Rosen, et al. Gemini 2.5: Pushing the frontier with advanced reasoning, multimodality, long context, and next generation agentic capabilities. *arXiv preprint arXiv:2507.06261*, 2025. 4, 6, 7
- [18] Matt Deitke, Dustin Schwenk, Jordi Salvador, Luca Weihs, Oscar Michel, Eli VanderBilt, Ludwig Schmidt, Kiana Ehsani, Aniruddha Kembhavi, and Ali Farhadi. Objaverse: A universe of annotated 3d objects. In *Proceedings of the IEEE/CVF conference on computer vision and pattern recognition*, pages 13142–13153, 2023. 2
- [19] Jiahua Dong and Yu-Xiong Wang. Vica-nerf: View-consistency-aware 3d editing of neural radiance fields. *Advances in Neural Information Processing Systems*, 36, 2024. 1, 7
- [20] Patrick Esser, Sumith Kulal, Andreas Blattmann, Rahim Entezari, Jonas Müller, Harry Saini, Yam Levi, Dominik Lorenz, Axel Sauer, Frederic Boesel, et al. Scaling rectified flow transformers for high-resolution image synthesis. In *Forty-first international conference on machine learning*, 2024. 5
- [21] Hyojun Go, Byeongjun Park, Jiho Jang, Jin-Young Kim, Soonwoo Kwon, and Changick Kim. Splatflow: Multi-view rectified flow model for 3d gaussian splatting synthesis. *arXiv preprint arXiv:2411.16443*, 2024. 7
- [22] Zheng Gu, Shiyuan Yang, Jing Liao, Jing Huo, and Yang Gao. Analogist: Out-of-the-box visual in-context learning

- with image diffusion model. *ACM Transactions on Graphics (TOG)*, 43(4):1–15, 2024. 1
- [23] Ayaan Haque, Matthew Tancik, Alexei A Efros, Aleksander Holynski, and Angjoo Kanazawa. Instruct-nerf2nerf: Editing 3d scenes with instructions. In *Proceedings of the IEEE/CVF International Conference on Computer Vision*, pages 19740–19750, 2023. 1, 2, 7
- [24] Wenyi Hong, Ming Ding, Wendi Zheng, Xinghan Liu, and Jie Tang. Cogvideo: Large-scale pretraining for text-to-video generation via transformers. *arXiv preprint arXiv:2205.15868*, 2022. 2
- [25] Yicong Hong, Kai Zhang, Jiuxiang Gu, Sai Bi, Yang Zhou, Difan Liu, Feng Liu, Kalyan Sunkavalli, Trung Bui, and Hao Tan. Lrm: Large reconstruction model for single image to 3d. *arXiv preprint arXiv:2311.04400*, 2023. 2
- [26] Edward J Hu, Yelong Shen, Phillip Wallis, Zeyuan Allen-Zhu, Yuanzhi Li, Shean Wang, Lu Wang, and Weizhu Chen. LoRA: Low-rank adaptation of large language models. In *International Conference on Learning Representations*, 2022. 2, 5
- [27] Jiahao Hu, Tianxiong Zhong, Xuebo Wang, Boyuan Jiang, Xingye Tian, Fei Yang, Pengfei Wan, and Di Zhang. Vivid-10m: A dataset and baseline for versatile and interactive video local editing. *arXiv preprint arXiv:2411.15260*, 2024. 4
- [28] Xu Hu, Yiyang Feng, Junran Peng, Jiawei He, Liyi Chen, Chuanchen Luo, Xucheng Yin, Qing Li, and Zhaoxiang Zhang. Marketgen: A scalable simulation platform with auto-generated embodied supermarket environments. *arXiv preprint arXiv:2511.21161*, 2025. 9
- [29] Binbin Huang, Zehao Yu, Anpei Chen, Andreas Geiger, and Shenghua Gao. 2d gaussian splatting for geometrically accurate radiance fields. In *SIGGRAPH 2024 Conference Papers*. Association for Computing Machinery, 2024. 5, 6
- [30] Lihan Jiang, Yucheng Mao, Linning Xu, Tao Lu, Kerui Ren, Yichen Jin, Xudong Xu, Mulin Yu, Jiangmiao Pang, Feng Zhao, et al. Anysplat: Feed-forward 3d gaussian splatting from unconstrained views. *arXiv preprint arXiv:2505.23716*, 2025. 2, 3
- [31] Xuan Ju, Weicai Ye, Quande Liu, Qiulin Wang, Xintao Wang, Pengfei Wan, Di Zhang, Kun Gai, and Qiang Xu. Fulldit: Multi-task video generative foundation model with full attention. *arXiv preprint arXiv:2503.19907*, 2025. 8
- [32] Heewoo Jun and Alex Nichol. Shap-e: Generating conditional 3d implicit functions. *arXiv preprint arXiv:2305.02463*, 2023. 2
- [33] Tero Karras, Miika Aittala, Timo Aila, and Samuli Laine. Elucidating the design space of diffusion-based generative models. *Advances in neural information processing systems*, 35:26565–26577, 2022. 3
- [34] Bernhard Kerbl, Georgios Kopanas, Thomas Leimkühler, and George Drettakis. 3d gaussian splatting for real-time radiance field rendering. *ACM Trans. Graph.*, 42(4):139–1, 2023. 1, 2
- [35] Peng Li, Suizhi Ma, Jialiang Chen, Yuan Liu, Congyi Zhang, Wei Xue, Wenhan Luo, Alla Sheffer, Wenping Wang, and Yike Guo. Cmd: Controllable multiview diffusion for 3d editing and progressive generation. In *Proceedings of the Special Interest Group on Computer Graphics and Interactive Techniques Conference Conference Papers*, pages 1–10, 2025. 2
- [36] Ruibin Li, Ruihuang Li, Song Guo, and Lei Zhang. Source prompt disentangled inversion for boosting image editability with diffusion models. In *European Conference on Computer Vision*, pages 404–421. Springer, 2024. 1
- [37] Ruihuang Li, Liyi Chen, Zhengqiang Zhang, Varun Jampani, Vishal M Patel, and Lei Zhang. Syncnoise: Geometrically consistent noise prediction for instruction-based 3d editing. In *Proceedings of the AAAI Conference on Artificial Intelligence*, pages 4905–4913, 2025. 2
- [38] Yunlong Lin, Zixu Lin, Kunjie Lin, Jinbin Bai, Panwang Pan, Chenxin Li, Haoyu Chen, Zhongdao Wang, Xinghao Ding, Wenbo Li, et al. Jarvisart: Liberating human artistic creativity via an intelligent photo retouching agent. *arXiv preprint arXiv:2506.17612*, 2025. 9
- [39] Yunlong Lin, Linqing Wang, Kunjie Lin, Zixu Lin, Kaixiong Gong, Wenbo Li, Bin Lin, Zhenxi Li, Shiyi Zhang, Yuyang Peng, et al. Jarvisevo: Towards a self-evolving photo editing agent with synergistic editor-evaluator optimization. *arXiv preprint arXiv:2511.23002*, 2025. 9
- [40] Lu Ling, Yichen Sheng, Zhi Tu, Wentian Zhao, Cheng Xin, Kun Wan, Lantao Yu, Qianyu Guo, Zixun Yu, Yawen Lu, et al. D13dv-10k: A large-scale scene dataset for deep learning-based 3d vision. In *Proceedings of the IEEE/CVF Conference on Computer Vision and Pattern Recognition*, pages 22160–22169, 2024. 4
- [41] Zhiheng Liu, Hao Ouyang, Qiuyu Wang, Ka Leong Cheng, Jie Xiao, Kai Zhu, Nan Xue, Yu Liu, Yujun Shen, and Yang Cao. Infusion: Inpainting 3d gaussians via learning depth completion from diffusion prior. *arXiv preprint arXiv:2404.11613*, 2024. 5
- [42] Ilya Loshchilov and Frank Hutter. Decoupled weight decay regularization. *arXiv preprint arXiv:1711.05101*, 2017. 5
- [43] Chaofan Luo, Donglin Di, Xun Yang, Yongjia Ma, Zhou Xue, Chen Wei, and Yebin Liu. Trame: Trajectory-anchored multi-view editing for text-guided 3d gaussian splatting manipulation. *arXiv preprint arXiv:2407.02034*, 2024. 1
- [44] Baorui Ma, Huachen Gao, Haoge Deng, Zhengxiong Luo, Tiejun Huang, Lulu Tang, and Xinlong Wang. You see it, you got it: Learning 3d creation on pose-free videos at scale. In *Proceedings of the Computer Vision and Pattern Recognition Conference*, pages 2016–2029, 2025. 7
- [45] Chenlin Meng, Yutong He, Yang Song, Jiaming Song, Jiajun Wu, Jun-Yan Zhu, and Stefano Ermon. Sdedit: Guided image synthesis and editing with stochastic differential equations. *arXiv preprint arXiv:2108.01073*, 2021. 4
- [46] Ben Mildenhall, Pratul P Srinivasan, Matthew Tancik, Jonathan T Barron, Ravi Ramamoorthi, and Ren Ng. Nerf: Representing scenes as neural radiance fields for view synthesis. *Communications of the ACM*, 65(1):99–106, 2021. 1, 2
- [47] Ashkan Mirzaei, Tristan Aumentado-Armstrong, Konstantinos G. Derpanis, Jonathan Kelly, Marcus A. Brubaker, Igor Gilitschenski, and Alex Levinshstein. SPIn-NeRF: Multiview

- segmentation and perceptual inpainting with neural radiance fields. In *CVPR*, 2023. 1, 2, 5, 6
- [48] Jingyi Pan, Dan Xu, and Qiong Luo. Diga3d: Coarse-to-fine diffusional propagation of geometry and appearance for versatile 3d inpainting. *arXiv preprint arXiv:2507.00429*, 2025. 2
- [49] Panwang Pan, Chenguo Lin, Jingjing Zhao, Chenxin Li, Yuchen Lin, Haopeng Li, Honglei Yan, Kairun Wen, Yunlong Lin, Yixuan Yuan, et al. Diff4splat: Controllable 4d scene generation with latent dynamic reconstruction models. *arXiv preprint arXiv:2511.00503*, 2025. 9
- [50] Zhangyang Qi, Yunhan Yang, Mengchen Zhang, Long Xing, Xiaoyang Wu, Tong Wu, Dahua Lin, Xihui Liu, Jiaqi Wang, and Hengshuang Zhao. Tailor3d: Customized 3d assets editing and generation with dual-side images, 2024. 2
- [51] Huaizhi Qu, Ruichen Zhang, Shuqing Luo, Luchao Qi, Zhihao Zhang, Xiaoming Liu, Roni Sengupta, and Tianlong Chen. Editcast3d: Single-frame-guided 3d editing with video propagation and view selection. *arXiv preprint arXiv:2510.13652*, 2025. 2
- [52] Jeremy Reizenstein, Roman Shapovalov, Philipp Henzler, Luca Sbordone, Patrick Labatut, and David Novotny. Common objects in 3d: Large-scale learning and evaluation of real-life 3d category reconstruction. In *International Conference on Computer Vision*, 2021. 4, 5, 6
- [53] Robin Rombach, Andreas Blattmann, Dominik Lorenz, Patrick Esser, and Björn Ommer. High-resolution image synthesis with latent diffusion models. In *Proceedings of the IEEE/CVF conference on computer vision and pattern recognition*, pages 10684–10695, 2022. 3
- [54] Ahmad Salimi, Tristan Aumentado-Armstrong, Marcus A Brubaker, and Konstantinos G Derpanis. Geometry-aware diffusion models for multiview scene inpainting. *arXiv preprint arXiv:2502.13335*, 2025. 3
- [55] Kyle Sargent, Zizhang Li, Tanmay Shah, Charles Herrmann, Hong-Xing Yu, Yunzhi Zhang, Eric Ryan Chan, Dmitry Lagun, Li Fei-Fei, Deqing Sun, et al. Zeronvs: Zero-shot 360-degree view synthesis from a single image. In *Proceedings of the IEEE/CVF Conference on Computer Vision and Pattern Recognition*, pages 9420–9429, 2024. 6
- [56] Roman Suvorov, Elizaveta Logacheva, Anton Mashikhin, Anastasia Remizova, Arsenii Ashukha, Aleksei Silvestrov, Naejin Kong, Harshith Goka, Kiwoong Park, and Victor Lempitsky. Resolution-robust large mask inpainting with fourier convolutions. In *Proceedings of the IEEE/CVF winter conference on applications of computer vision*, pages 2149–2159, 2022. 5
- [57] Jiale Tao, Yanbing Zhang, Qixun Wang, Yiji Cheng, Haofan Wang, Xu Bai, Zhengguang Zhou, Ruihuang Li, Linqing Wang, Chunyu Wang, et al. Instantcharacter: Personalize any characters with a scalable diffusion transformer framework. *arXiv preprint arXiv:2504.12395*, 2025. 1
- [58] Zeng Tao, Zheng Ding, Zeyuan Chen, Xiang Zhang, Leizhi Li, and Zhuowen Tu. C3editor: Achieving controllable consistency in 2d model for 3d editing. *arXiv preprint arXiv:2510.04539*, 2025. 3
- [59] Team Wan, Ang Wang, Baole Ai, Bin Wen, Chaojie Mao, Chen-Wei Xie, Di Chen, Feiwu Yu, Haiming Zhao, Jianxiao Yang, Jianyuan Zeng, Jiayu Wang, Jingfeng Zhang, Jingren Zhou, Jinkai Wang, Jixuan Chen, Kai Zhu, Kang Zhao, Keyu Yan, Lianghua Huang, Mengyang Feng, Ningyi Zhang, Pandeng Li, Pingyu Wu, Ruihang Chu, Ruili Feng, Shiwei Zhang, Siyang Sun, Tao Fang, Tianxing Wang, Tianyi Gui, Tingyu Weng, Tong Shen, Wei Lin, Wei Wang, Wei Wang, Wenmeng Zhou, Wenten Wang, Wenting Shen, Wenyuan Yu, Xianzhong Shi, Xiaoming Huang, Xin Xu, Yan Kou, Yangyu Lv, Yifei Li, Yijing Liu, Yiming Wang, Yingya Zhang, Yitong Huang, Yong Li, You Wu, Yu Liu, Yulin Pan, Yun Zheng, Yuntao Hong, Yupeng Shi, Yutong Feng, Zeyinzi Jiang, Zhen Han, Zhi-Fan Wu, and Ziyu Liu. Wan: Open and advanced large-scale video generative models. *arXiv preprint arXiv:2503.20314*, 2025. 2
- [60] Can Wang, Menglei Chai, Mingming He, Dongdong Chen, and Jing Liao. Clip-nerf: Text-and-image driven manipulation of neural radiance fields. In *Proceedings of the IEEE/CVF conference on computer vision and pattern recognition*, pages 3835–3844, 2022. 2
- [61] Can Wang, Ruixiang Jiang, Menglei Chai, Mingming He, Dongdong Chen, and Jing Liao. Nerf-art: Text-driven neural radiance fields stylization. *IEEE Transactions on Visualization and Computer Graphics*, 2023. 2
- [62] Jianyuan Wang, Minghao Chen, Nikita Karaev, Andrea Vedaldi, Christian Rupprecht, and David Novotny. Vggt: Visual geometry grounded transformer. In *Proceedings of the Computer Vision and Pattern Recognition Conference*, pages 5294–5306, 2025. 2, 3
- [63] Pengfei Wang, Liyi Chen, Zhiyuan Ma, Yanjun Guo, Guowen Zhang, and Lei Zhang. One2scene: Geometric consistent explorable 3d scene generation from a single image. *arXiv preprint arXiv:2602.19766*, 2026. 5
- [64] Ruicheng Wang, Sicheng Xu, Cassie Dai, Jianfeng Xiang, Yu Deng, Xin Tong, and Jiaolong Yang. Moge: Unlocking accurate monocular geometry estimation for open-domain images with optimal training supervision. In *Proceedings of the Computer Vision and Pattern Recognition Conference*, pages 5261–5271, 2025. 7
- [65] Yuxin Wang, Qianyi Wu, Guofeng Zhang, and Dan Xu. Gscream: Learning 3d geometry and feature consistent gaussian splatting for object removal. In *ECCV*, 2024. 5, 6
- [66] Yuxuan Wang, Xuanyu Yi, Zike Wu, Na Zhao, Long Chen, and Hanwang Zhang. View-consistent 3d editing with gaussian splatting. In *European conference on computer vision*, pages 404–420. Springer, 2024. 1, 2
- [67] Kairun Wen, Yuzhi Huang, Runyu Chen, Hui Zheng, Yunlong Lin, Panwang Pan, Chenxin Li, Wenyan Cong, Jian Zhang, Junbin Lu, et al. Dynamicverse: A physically-aware multimodal framework for 4d world modeling. *arXiv preprint arXiv:2512.03000*, 2025. 9
- [68] Minghao Wen, Shengjie Wu, Kangkan Wang, and Dong Liang. Intersedit: Interactive 3d gaussian splatting editing with 3d geometry-consistent attention prior. *arXiv preprint arXiv:2507.04961*, 2025. 1
- [69] Chenfei Wu, Jiahao Li, Jingren Zhou, Junyang Lin, Kaiyuan Gao, Kun Yan, Sheng ming Yin, Shuai Bai, Xiao Xu, Yilei Chen, Yuxiang Chen, Zecheng Tang, Zekai Zhang, Zhengyi

- Wang, An Yang, Bowen Yu, Chen Cheng, Dayiheng Liu, Deqing Li, Hang Zhang, Hao Meng, Hu Wei, Jingyuan Ni, Kai Chen, Kuan Cao, Liang Peng, Lin Qu, Minggang Wu, Peng Wang, Shuting Yu, Tingkun Wen, Wensen Feng, Xiaoxiao Xu, Yi Wang, Yichang Zhang, Yongqiang Zhu, Yujia Wu, Yuxuan Cai, and Zenan Liu. Qwen-image technical report, 2025. [2](#), [3](#), [4](#)
- [70] Chung-Ho Wu, Yang-Jung Chen, Ying-Huan Chen, Jie-Ying Lee, Bo-Hsu Ke, Chun-Wei Tuan Mu, Yi-Chuan Huang, Chin-Yang Lin, Min-Hung Chen, Yen-Yu Lin, et al. Aurafusion360: Augmented unseen region alignment for reference-based 360deg unbounded scene inpainting. In *Proceedings of the Computer Vision and Pattern Recognition Conference*, pages 16366–16376, 2025. [5](#), [6](#), [8](#)
- [71] Jing Wu, Jia-Wang Bian, Xinghui Li, Guangrun Wang, Ian Reid, Philip Torr, and Victor Adrian Prisacariu. Gaussctrl: multi-view consistent text-driven 3d gaussian splatting editing. *arXiv preprint arXiv:2403.08733*, 2024. [2](#)
- [72] Yuhui Wu, Chenxi Xie, Ruibin Li, Liyi Chen, Qiaosi Yi, and Lei Zhang. Cocoedit: Content-consistent image editing via region regularized reinforcement learning. *arXiv preprint arXiv:2602.14068*, 2026. [1](#)
- [73] Hongchi Xia, Yang Fu, Sifei Liu, and Xiaolong Wang. Rgb-d objects in the wild: Scaling real-world 3d object learning from rgb-d videos. In *Proceedings of the IEEE/CVF Conference on Computer Vision and Pattern Recognition*, pages 22378–22389, 2024. [4](#)
- [74] Shiyuan Yang, Xiaodong Chen, and Jing Liao. Uni-paint: A unified framework for multimodal image inpainting with pretrained diffusion model. In *Proceedings of the 31st ACM International Conference on Multimedia*, pages 3190–3199, 2023. [1](#)
- [75] Shiyuan Yang, Liang Hou, Haibin Huang, Chongyang Ma, Pengfei Wan, Di Zhang, Xiaodong Chen, and Jing Liao. Direct-a-video: Customized video generation with user-directed camera movement and object motion. In *ACM SIGGRAPH 2024 Conference Papers*, pages 1–12, 2024. [2](#)
- [76] Shiyuan Yang, Ruihuang Li, Jiale Tao, Shuai Shao, Qinglin Lu, and Jing Liao. Effectmaker: Unifying reasoning and generation for customized visual effect creation. *arXiv preprint arXiv:2603.06014*, 2026.
- [77] Zhuoyi Yang, Jiayan Teng, Wendi Zheng, Ming Ding, Shiyu Huang, Jiazheng Xu, Yuanming Yang, Wenyi Hong, Xiaohan Zhang, Guanyu Feng, et al. Cogvideox: Text-to-video diffusion models with an expert transformer. *arXiv preprint arXiv:2408.06072*, 2024. [2](#)
- [78] Junliang Ye, Shenghao Xie, Ruowen Zhao, Zhengyi Wang, Hongyu Yan, Wenqiang Zu, Lei Ma, and Jun Zhu. Nano3d: A training-free approach for efficient 3d editing without masks. *arXiv preprint arXiv:2510.15019*, 2025. [2](#)
- [79] Mingqiao Ye, Martin Danelljan, Fisher Yu, and Lei Ke. Gaussian grouping: Segment and edit anything in 3d scenes. In *ECCV*, 2024. [5](#), [6](#)
- [80] Wangbo Yu, Jinbo Xing, Li Yuan, Wenbo Hu, Xiaoyu Li, Zhipeng Huang, Xiangjun Gao, Tien-Tsin Wong, Ying Shan, and Yonghong Tian. Viewcrafter: Taming video diffusion models for high-fidelity novel view synthesis. *arXiv preprint arXiv:2409.02048*, 2024. [5](#), [8](#)
- [81] Guowen Zhang, Junsong Fan, Liyi Chen, Zhaoxiang Zhang, Zhen Lei, and Lei Zhang. General geometry-aware weakly supervised 3d object detection. In *European Conference on Computer Vision*, pages 290–309. Springer, 2024. [4](#)
- [82] Guowen Zhang, Lue Fan, Chenhang He, Zhen Lei, Zhaoxiang Zhang, and Lei Zhang. Voxel mamba: Group-free state space models for point cloud based 3d object detection. *Advances in Neural Information Processing Systems*, 37:81489–81509, 2024. [1](#)
- [83] Guowen Zhang, Chenhang He, Liyi Chen, and Lei Zhang. Bevdilation: Lidar-centric multi-modal fusion for 3d object detection. *arXiv preprint arXiv:2512.02972*, 2025. [4](#), [9](#)
- [84] Kai Zhang, Sai Bi, Hao Tan, Yuanbo Xiangli, Nanxuan Zhao, Kalyan Sunkavalli, and Zexiang Xu. Gs-lrm: Large reconstruction model for 3d gaussian splatting. In *European Conference on Computer Vision*, pages 1–19. Springer, 2024. [2](#)
- [85] Yanming Zhang, Jun-Kun Chen, Jipeng Lyu, and Yu-Xiong Wang. V2edit: Versatile video diffusion editor for videos and 3d scenes. *arXiv preprint arXiv:2503.10634*, 2025. [2](#)
- [86] Zechuan Zhang, Ji Xie, Yu Lu, Zongxin Yang, and Yi Yang. Enabling instructional image editing with in-context generation in large scale diffusion transformer. In *The Thirty-ninth Annual Conference on Neural Information Processing Systems*. [7](#)
- [87] Canyu Zhao, Xiaoman Li, Tianjian Feng, Zhiyue Zhao, Hao Chen, and Chunhua Shen. Tinker: Diffusion’s gift to 3d-multi-view consistent editing from sparse inputs without per-scene optimization. *arXiv preprint arXiv:2508.14811*, 2025. [3](#)
- [88] Yang Zheng, Mengqi Huang, Nan Chen, and Zhendong Mao. Pro3d-editor: A progressive-views perspective for consistent and precise 3d editing. *arXiv preprint arXiv:2506.00512*, 2025. [3](#)
- [89] Jensen (Jinghao) Zhou, Hang Gao, Vikram Voleti, Aaryaman Vasishtha, Chun-Han Yao, Mark Boss, Philip Torr, Christian Rupprecht, and Varun Jampani. Stable virtual camera: Generative view synthesis with diffusion models. *arXiv preprint arXiv:2503.14489*, 2025. [2](#), [3](#), [4](#), [5](#)
- [90] Jingyu Zhuang, Chen Wang, Liang Lin, Lingjie Liu, and Guanbin Li. Dreameditor: Text-driven 3d scene editing with neural fields. In *SIGGRAPH Asia 2023 Conference Papers*, pages 1–10, 2023. [2](#)

Supplementary File to “Omni-3DEdit: Generalized Versatile 3D Editing in One-Pass”

This supplementary file provides the following materials:

- **Additional Training Data Details** (referring to Sec. S1);
- **Attention Visualization** (referring to Sec. S2);
- **Additional Testing Data Details** (referring to Sec. S3).

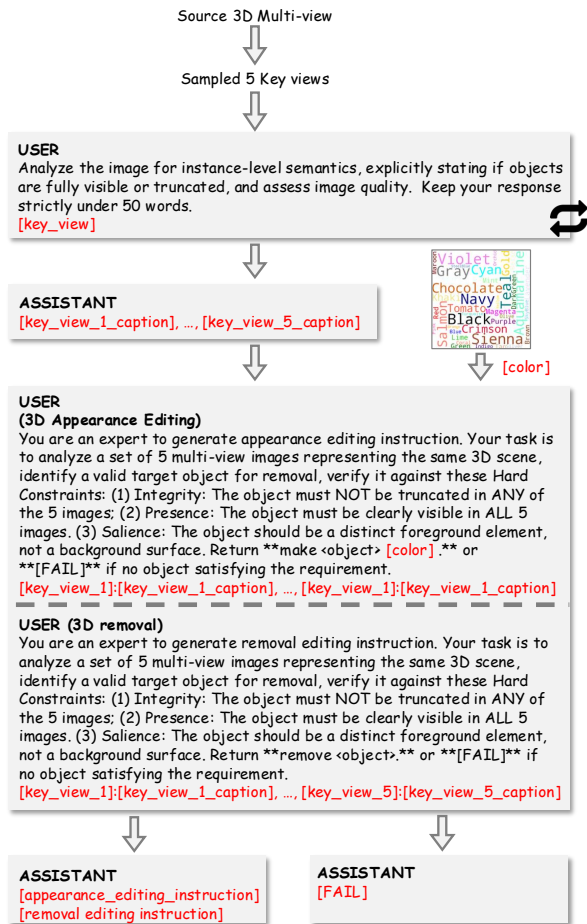


Figure S1. System prompts for instruction generation.

S1. Additional Training Data Details

In the main paper, we briefly described the four stages of our data curation pipeline. In this section, we provide more comprehensive implementation details.

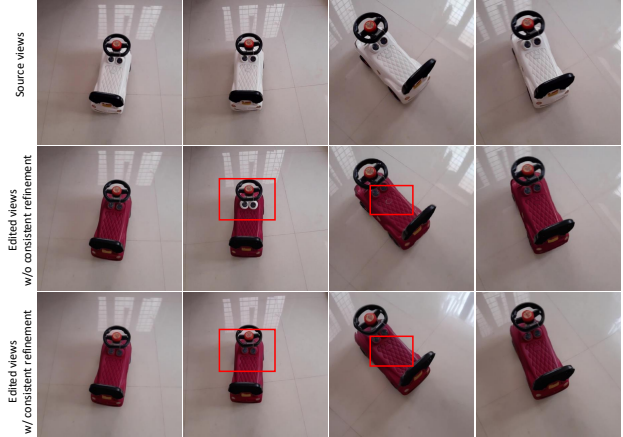


Figure S2. Comparison of per-view editing and consistent refinement. Consistent refinement eliminates the minor inconsistencies that occur on per-view appearance editing.

Instruction Generation. We employ a locally deployed Qwen2.5-VL-32B [10] model together with the Gemini-2.5 Pro [3] API to generate appearance editing and object removal instructions based on the provided multi-view images. Given that processing an excessive number of views increases computational complexity and reduces inference speed, we randomly sample five views per scene as input for the model. Furthermore, to enhance multimodal reasoning capabilities, we first utilize VLM to describe the content of each image before determining the final editing instruction, which takes full advantage of the reasoning capability in the texture space. Regarding appearance editing, we observe that the model tends to generate repetitive colors (*e.g.*, frequently outputting “black”), resulting in limited diversity. To address this, we establish a pre-defined color bank and specify a randomly sampled color for each appearance editing directly, significantly improving the diversity of the generated appearance editing instructions. The complete system prompts are provided in Fig. S1.

Consistent Refinement. We observe that 3D appearance editing typically introduces minimal geometric deformation, while 3D object removal often results in backgrounds with smooth, regular geometry (*e.g.*, flat ground). Conse-

Prompt for vLLM-based Quality Filter

```

### Role Definition
You are a strict 3D Computer Vision Quality Assurance Expert. Your mission is to evaluate the success of a 3D scene editing task by comparing source 3D multi-view inputs with edited 3D multi-view outputs, based on a specific instruction.

### Evaluation Protocol
You must strictly follow this two-stage reasoning process before delivering a final verdict.

**Stage 1: Per-View Independent Verification**
Iterate through EACH view pair (Source View vs. Edited View) and verify:
1. **Instruction Adherence:** Does the specific view clearly reflect the requested edit? (e.g., Is the object removed? Did the color change?)
2. **Background Preservation:** Are the non-edited regions (background, other objects) identical to the source view? (Look for unwanted changes or hallucinations).
3. **Image Quality:** Is the edited view free from severe artifacts like blurring, holes, or in-painting noise?

**Stage 2: Cross-View Consistency Check**
Analyze the <edited 3D multi-view> images as a holistic 3D sequence:
1. **Geometric Consistency:** Does the edited object maintain a rigid 3D shape across all views? (Reject if the object shape morphs, stretches, or "drifts" between angles).
2. **Texture/Color Consistency:** Is the appearance uniform across different viewing angles? (e.g., The car shouldn't be red in View 1 but orange in View 4).

### Failure Conditions (Automatic Fail)
Return `[FAIL]` immediately if ANY of the following are true:
- The edit is missing in one or more views.
- The object looks 3D-inconsistent (e.g., Janus problem, shape-shifting).
- Significant artifacts or background corruption are present.

### Output Format
You must provide your analysis followed by the final decision:

**Stage 1 Analysis:** [Briefly confirm if each view matches the instruction and preserves background]
**Stage 2 Analysis:** [Briefly assess geometric and texture consistency across views]
**Conclusion:** [PASS] or [FAIL]

```

Figure S3. **System prompts for quality filter.** Firstly, evaluation is conducted on per source-edited views to ensure that the instruction has been successfully executed. Then, a subjectively multi-view consistent evaluation is conducted to filter cases with obvious inconsistency.

quently, even with per-frame editing, both appearance editing and removal tasks will introduce minor 3D inconsistencies manifesting as color variations or high-frequency texture artifacts. These discrepancies can be mitigated through techniques such as iterative 2D-3D-2D refinement [1, 2, 4, 6]. However, we eschew multi-round iterative refinement during our data generation phase, as this process is prohibitively time-consuming (~ 10 minutes per scene) and hinders scalable data curation. Instead, drawing inspiration from SDEdit [8], we randomly select an edited view to serve as the conditional view. For the remaining views, we add a small amount of noise and perform EDM denoising using the pre-trained SEVA model. This streamlined process requires ~ 20 seconds per scene, significantly reducing the time overhead for data construction. In the inference (denoising) stage, SEVA denoises the noisy target view latent x_t with the EDM solver [5] as follows¹:

$$x_t = x_{t+1} + \frac{\sigma_t - \sigma_{t+1}}{\sigma_{t+1}} (x_{t+1} - D_\theta(x_{t+1}, t+1; I)), \quad (\text{S1})$$

where σ_t is the scheduled noise level at step $t \in [0, T]$. $D_\theta(x_t, t; I)$ is the estimated x_0 from x_t conditioned on the

¹For simplicity, we omit the 2nd order correction. The noise level increases with the step t , which is opposite to the original paper [5].

first frame I , which is defined as follows:

$$D_\theta(x_t, t; I) = x_t - (c_{skip}^t x_t + c_{out}^t F_\theta(c_{in}^t x_t, c_{noise}^t; I)), \quad (\text{S2})$$

where c_{skip}^t , c_{in}^t , c_{out}^t , and c_{noise}^t are coefficients of the noise schedule in EDM.

Fig. S2 visualizes an example to demonstrate the effectiveness of our consistency refinement method. During the process of converting a white car to a red car by invoking Qwen-Image [9] on a per-view basis, local inconsistencies arise; for instance, the regions surrounding the two black circles in the second column are not turned red. Our consistency refinement successfully rectifies these discrepancies, yielding a highly consistent editing result.

Quality Filter. Fig. S3 provides a detailed illustration of the quality filtering process. We employ the Qwen2.5-VL-32B [10] to verify whether the edited images align with the editing instructions relative to the original images, ensuring that irrelevant regions remain largely unchanged and the image quality is not degraded by editing. Subsequently, we employ the VLM to subjectively assess the multi-view consistency, filtering out samples with significant discrepancies that cannot be rectified through consistency refinement.

Fig. S4 visualizes some examples to demonstrate data curation results. On the left, we display successful cases that pass all the four curation stages, including the final

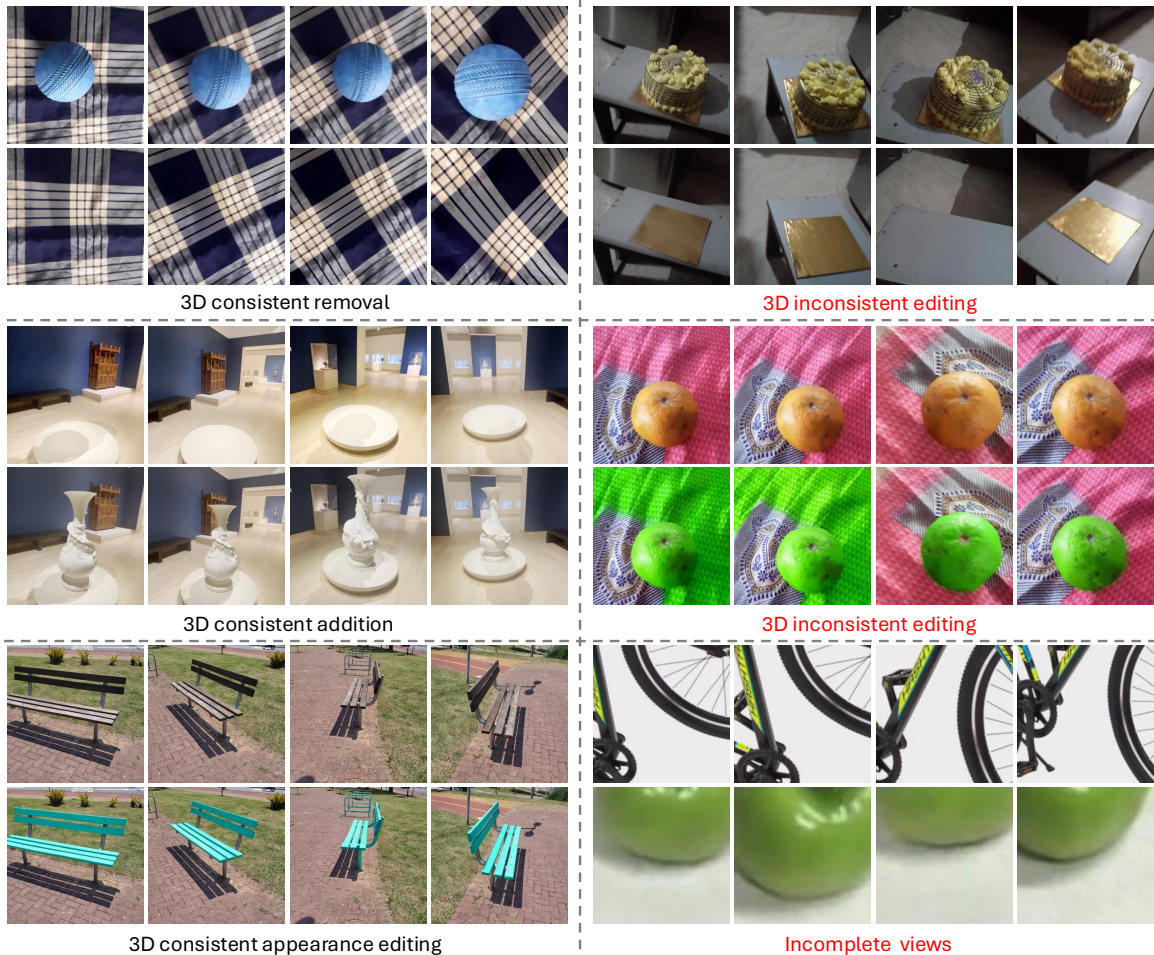


Figure S4. **Visualization of successful cases and failed cases.** We present several training data on the left and some failed cases on the right, which are caused by the inconsistent editing and incomplete views.

quality filter. On the right, we show some failure cases. In case 1, the cardboard at the base of the cake was not correctly removed in certain views. In case 2, large areas of the table-cloth were erroneously colored green during the process of changing the orange to green. These two cases exhibit significant erroneous regions that could not be corrected by consistency refinement, and they are consequently dropped during quality filtering. Additionally, case 3 is also discarded during the instruction generation phase due to dataset limitations or cropping issues, where the views do not contain the complete object and cannot be recognized by VLM.

Training Settings. We train Omni-3DEdit using the AdamW [7] optimizer with $\beta_1 = 0.9$, $\beta_2 = 0.999$, and a weight decay of 0.01. The training process utilizes a fixed learning rate of 1×10^{-4} and a batch size of 32 for a total of 4,000 training steps. Following the setting of SEVA [11] training setup, we employ the EpsWeight loss

Table S1. **Training settings and hyperparameters.**

config	value
optimizer	AdamW
base learning rate	1e-4
weight decay	0.01
eps	1e-8
optimizer momentum	$\beta_1, \beta_2 = 0.9, 0.999$
batch size	32
learning rate schedule	ConstantLR
training steps	4K
loss weight	EpsWeight
snr shift	2.4
CFG	1.2
UCG rate	0.2

strategy but omit weighting from camera distance. Furthermore, we adopt an SNR shift of 2.4 to improve the signal-to-noise ratio scheduling. For classifier-free guidance (CFG), we apply a condition dropout rate (UCG rate) of 0.2 during

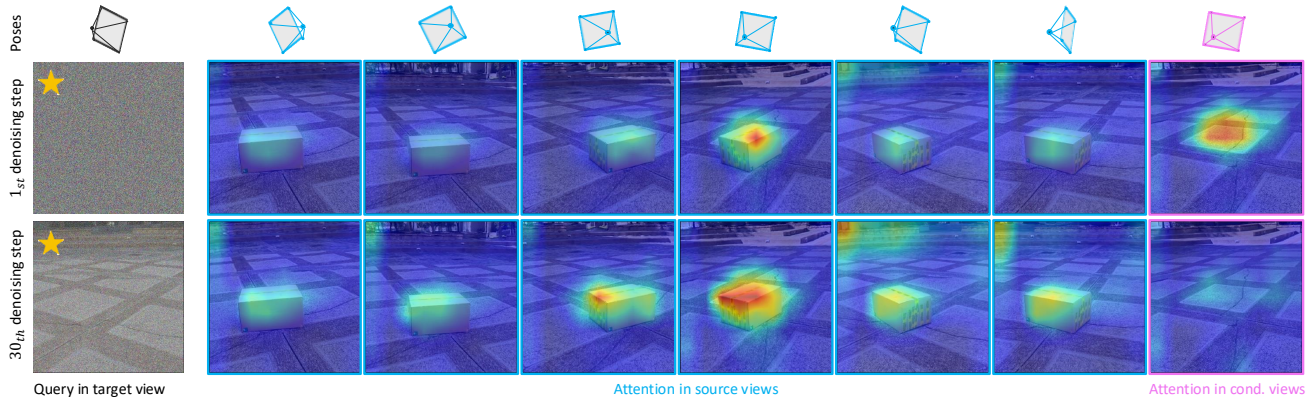


Figure S5. **Attention visualization of OmniNet Block during different denoising stages.** Omni-3DEdit can capture corresponding regions from source and conditional views based on the given camera poses. Pentagram is placed on the query regions.

Scene	Edit Instruction	Source Prompt	Target Prompt
Bear	“Turn it into a black bear.”	“A bear in the park.”	“A black bear in the park.”
Bear	“Remove the bear.”	“A bear in the park.”	“A plain stone in the park.”
Book	“Remove the book + add an apple.”	“A table with a book.”	“A table with an apple.”
Spinnerf_1	“Remove the trash + add a poster.”	“A trash on the ground.”	“A poster.”
Spinnerf_2	“Remove the box under tree.”	“A box under the tree.”	“A tree.”
CO3D.Keyboard	“Make the keyboard green + add a bottle.”	“A keyboard on the table.”	“A green keyboard and a bottle on the table.”
Garden	“Remove the vase.”	“A vase in the garden.”	“A wooden table in the garden.”
Garden	“Make the table blue.”	“A table.”	“A blue table.”
Spinnerf_7	“Remove the white object + add a plant.”	“A kettle on bench.”	“A plant on the bench.”
Bicycle	“Make the bicycle golden.”	“A bicycle on the glass.”	“A golden bicycle on the glass.”

Table S2. **The scene and instruction prompts in the datasets.**

training and use a guidance scale of 1.2 during inference.

S2. Attention Visualization

To probe how different views are leveraged during denoising, we visualize the attention distribution across distinct denoising stages. As illustrated in Fig. S5, we randomly select a target view and analyze the attention map corresponding to its top-left region within the multi-view attention block. At the initial denoising step (1st step), the query region predominantly attends to areas exhibiting significant discrepancies between the reference and source views, *a.k.a.*, regions of boxes present and absent. Notably, the source view aligned with the reference view’s camera pose garners the highest attention. This facilitates model’s interpretation of the intended task (3D removal) and the target object. At the 30th denoising step, the focused regions broaden beyond attending to the box’s location across all source views, and it explicitly attends to regions in the original views that are geometrically coincident with the selected top-left position. This suggests that such source geometric textures are effectively preserved by Omni-3DEdit. These findings validate Omni-3DEdit’s ability to utilize camera poses for resolving inter-view geometric relationships and

precisely localizing relevant content from source views.

S3. Additional Test Data Details

We present more details of our manually constructed cases in Tab. S2. These cases encompass standard appearance editing instructions to align with prior methodologies, such as ‘Turn it into a black bear’. Furthermore, we introduce more complex editing instructions, such as sequentially modifying an object’s color before adding an additional object to the scene. As discussed in the main text, these composite instructions not only rely on the model’s generalization capabilities but also necessitate high-fidelity results to support multi-round editing—a task that remains challenging for existing approaches.

Gemini Score. We employ evaluation criteria similar to those used in our quality filter, tasking Gemini-2.5 Pro [3] with assessing both the success of the multi-view editing and the maintenance of multi-view consistency. As shown in Fig. S6, we instruct Gemini to give a score from 1 to 5 by considering the editing instruction faithfulness, multi-view consistency, and visual quality comprehensively.

Prompt for Gemini Score

Role

You are an expert evaluator for 3D-aware image editing tasks. Your goal is to assess the quality of edited multi-view images based on an editing instruction.

Input Data

1. **Source Views**: Original images of the object.
2. **Edited Views**: Edited images of the object.
3. **Instruction**: The text description of the desired edit.

Evaluation Criteria

Please analyze the results based on the following three dimensions:

1. **Editing Adherence**: Did the edit strictly follow the instruction? (e.g., correct color, object addition/removal).
2. **Multi-View Consistency (Critical)**: Does the edited views appear 3D geometrically consistent across all viewpoints?
3. **Image Quality**: Are the images clear, sharp, and free of artifacts?

Output Format

You must structure your response strictly as follows. Provide a brief analysis for each dimension, followed by the final score.

Analysis

1. **Editing Adherence**: [Provide your analysis here. Did the model follow the instruction?]
2. **Multi-View Consistency**: [Provide your analysis here. Are there any inconsistencies between views?]
3. **Image Quality**: [Provide your analysis here. Are there any artifacts?]

Final Score

[Output a single integer from 1 to 5, where 1 is the worst and 5 is the best]

Figure S6. System prompts for gemini score.

References

- [1] Minghao Chen, Iro Laina, and Andrea Vedaldi. Dge: Direct gaussian 3d editing by consistent multi-view editing. In *European Conference on Computer Vision*, pages 74–92. Springer, 2024.
- [2] Yiwen Chen, Zilong Chen, Chi Zhang, Feng Wang, Xiaofeng Yang, Yikai Wang, Zhongang Cai, Lei Yang, Huaping Liu, and Guosheng Lin. Gaussianeditor: Swift and controllable 3d editing with gaussian splatting. In *Proceedings of the IEEE/CVF Conference on Computer Vision and Pattern Recognition*, pages 21476–21485, 2024.
- [3] Gheorghe Comanici, Eric Bieber, Mike Schaekermann, Ice Pasapat, Noveen Sachdeva, Inderjit Dhillon, Marcel Blisstein, Ori Ram, Dan Zhang, Evan Rosen, et al. Gemini 2.5: Pushing the frontier with advanced reasoning, multimodality, long context, and next generation agentic capabilities. *arXiv preprint arXiv:2507.06261*, 2025.
- [4] Jiahua Dong and Yu-Xiong Wang. Vica-nerf: View-consistency-aware 3d editing of neural radiance fields. *Advances in Neural Information Processing Systems*, 36, 2024.
- [5] Tero Karras, Miika Aittala, Timo Aila, and Samuli Laine. Elucidating the design space of diffusion-based generative models. *Advances in neural information processing systems*, 35:26565–26577, 2022.
- [6] Ruihuang Li, Liyi Chen, Zhengqiang Zhang, Varun Jampani, Vishal M Patel, and Lei Zhang. Synnoise: Geometrically consistent noise prediction for text-based 3d scene editing. *arXiv preprint arXiv:2406.17396*, 2024.
- [7] Ilya Loshchilov and Frank Hutter. Decoupled weight decay regularization. *arXiv preprint arXiv:1711.05101*, 2017.
- [8] Chenlin Meng, Yutong He, Yang Song, Jiaming Song, Jiajun Wu, Jun-Yan Zhu, and Stefano Ermon. Sdedit: Guided image synthesis and editing with stochastic differential equations. *arXiv preprint arXiv:2108.01073*, 2021.
- [9] Chenfei Wu, Jiahao Li, Jingren Zhou, Junyang Lin, Kaiyuan Gao, Kun Yan, Sheng ming Yin, Shuai Bai, Xiao Xu, Yilei Chen, Yuxiang Chen, Zecheng Tang, Zekai Zhang, Zhengyi Wang, An Yang, Bowen Yu, Chen Cheng, Dayiheng Liu, Deqing Li, Hang Zhang, Hao Meng, Hu Wei, Jingyuan Ni, Kai Chen, Kuan Cao, Liang Peng, Lin Qu, Minggang Wu, Peng Wang, Shuting Yu, Tingkun Wen, Wensen Feng, Xiaoxiao Xu, Yi Wang, Yichang Zhang, Yongqiang Zhu, Yujia Wu, Yuxuan Cai, and Zenan Liu. Qwen-image technical report, 2025.
- [10] An Yang, Baosong Yang, Binyuan Hui, Bo Zheng, Bowen Yu, Chang Zhou, Chengpeng Li, Chengyuan Li, Dayiheng Liu, Fei Huang, Guanting Dong, Haoran Wei, Huan Lin, Jialong Tang, Jialin Wang, Jian Yang, Jianhong Tu, Jianwei Zhang, Jianxin Ma, Jin Xu, Jingren Zhou, Jinze Bai, Jinzheng He, Junyang Lin, Kai Dang, Keming Lu, Keqin Chen, Kexin Yang, Mei Li, Mingfeng Xue, Na Ni, Pei Zhang, Peng Wang, Ru Peng, Rui Men, Ruize Gao, Runji Lin, Shijie Wang, Shuai Bai, Sinan Tan, Tianhang Zhu, Tianhao Li, Tianyu Liu, Wenbin Ge, Xiaodong Deng, Xiaohuan Zhou, Xingzhang Ren, Xinyu Zhang, Xipin Wei, Xuancheng Ren, Yang Fan, Yang Yao, Yichang Zhang, Yu Wan, Yunfei Chu, Yuqiong Liu, Zeyu Cui, Zhenru Zhang, and Zhihao Fan.

Qwen2 technical report. *arXiv preprint arXiv:2407.10671*, 2024.

- [11] Jensen (Jinghao) Zhou, Hang Gao, Vikram Voleti, Aaryaman Vasishtha, Chun-Han Yao, Mark Boss, Philip Torr, Christian Rupprecht, and Varun Jampani. Stable virtual camera: Generative view synthesis with diffusion models. *arXiv preprint arXiv:2503.14489*, 2025.